



Supplement of

Data assimilation of CrIS NH₃ satellite observations for improving spatiotemporal NH₃ distributions in LOTOS-EUROS

Shelley van der Graaf et al.

Correspondence to: Shelley van der Graaf (s.c.vander.graaf@vu.nl)

The copyright of individual parts of the supplement might differ from the article licence.

5

Supplementary material

10

S.1 Local Ensemble Transform Kalman Filter setting experiments

Two experiments were performed to study the effect of the LETKF filter settings in more detail. In the first experiment homogeneous NH_3 emission fields were used to study the possible emission adjustments that can be achieved by the LETKF. In this experiment, the NH_3 base emissions at every grid cell were set to two times the mean NH_3 emissions in the Netherlands. The NH_3 time factors were kept time-invariant, i.e., set to 1 throughout the year. For different LETKF filter settings, the obtained emission perturbation factors β are shown in Fig. S22 and Fig. S23. The experiment shows that increasing temporal length scale τ , i.e., prolonging the time an emission update computed by the LETKF is kept in the model, leads to a larger distribution of computed β factors. Imposing more noise on the ensemble members, i.e., a σ value to 1 instead of 0.5, also leads to a larger distribution in β factors, as well as an overall increase in β factors. The average computed β factors illustrate that large-scale spatial patterns in NH_3 concentrations, as observed by the CrIS instrument, can be resolved. The distribution of the obtained β factors is, except for March, very similar throughout the year. This illustrates that the LETKF is unable to resolve temporal patterns well without sensible initial inputs. In the second experiment the effect of temporal length scale τ is studied in more detail. In this experiment, our initial model setup was kept, but the temporal length scale is extended to $\tau = 10$ days and $\tau = 14$ days. The obtained β factors are shown in Fig. S24 and Fig. S25. The spatial pattern of the obtained β factors remained very similar in all model runs, however, the range in β factors increased with increasing τ . Moreover, as patterns of the CrIS- NH_3 observations is followed more strongly with increasing τ values, the obtained spatial variation in β factors became more distinct.

30

Mean NH_4 wet deposition (2014-2018)

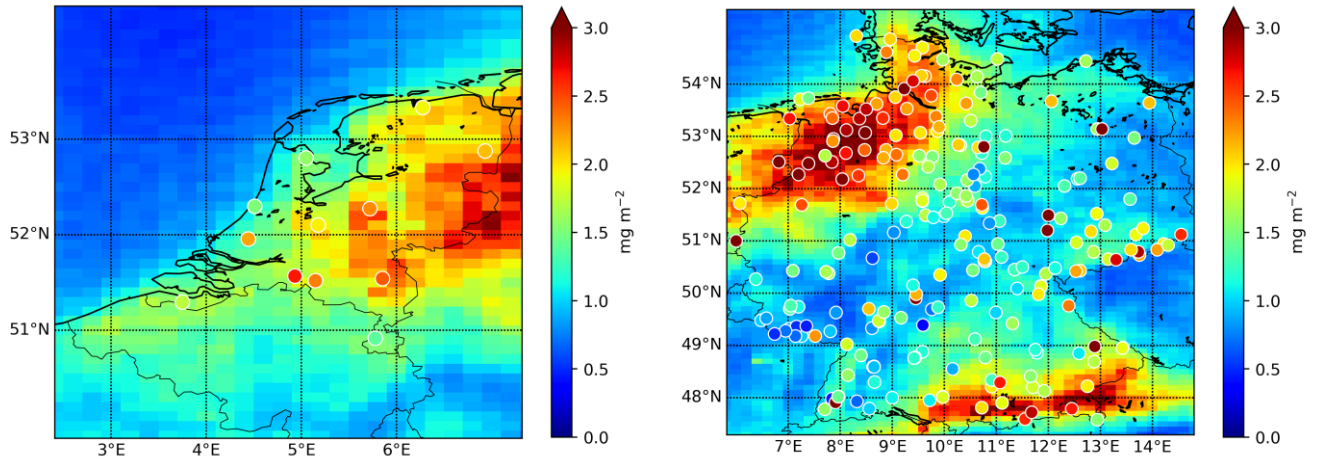


Figure S1: Locations of the wet-only samplers used in this study, plotted on top of the modelled mean NH_4 wet deposition in 2014 to 2018.

Scaling factor applied for high emission pixels ($> 0.0025 \text{ kg NH}_3 \text{ m}^{-2} \text{ yr}^{-1}$) in 2014

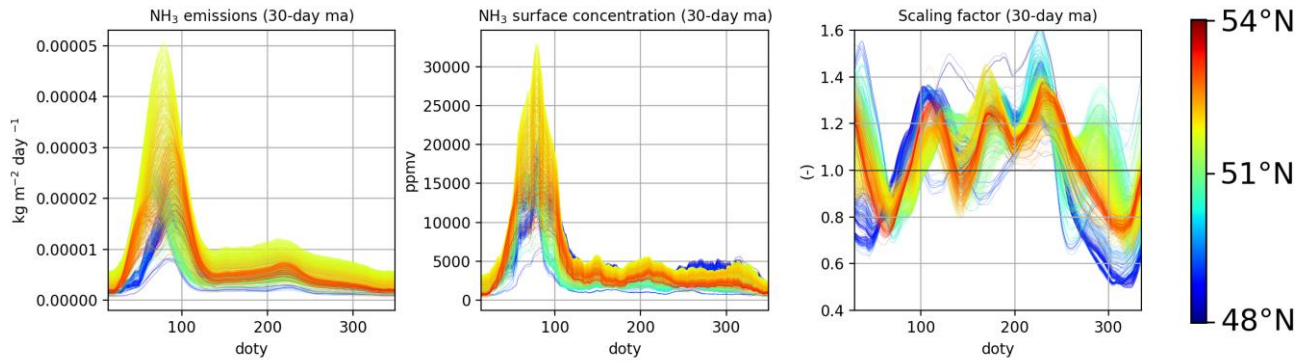
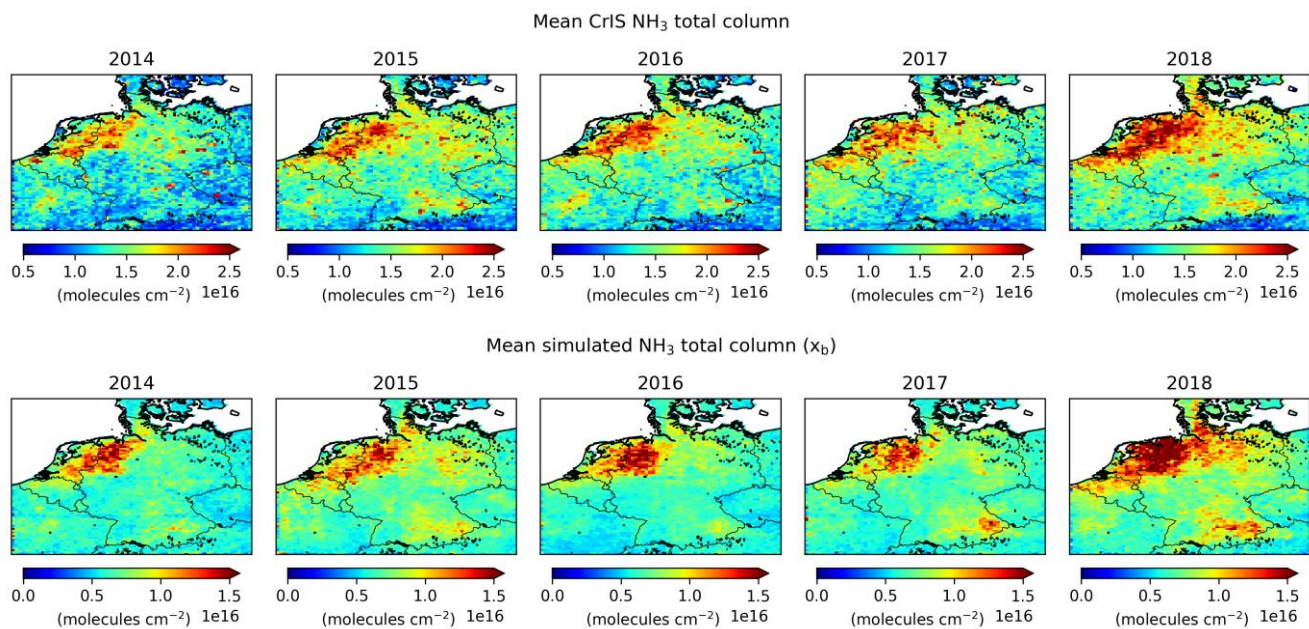
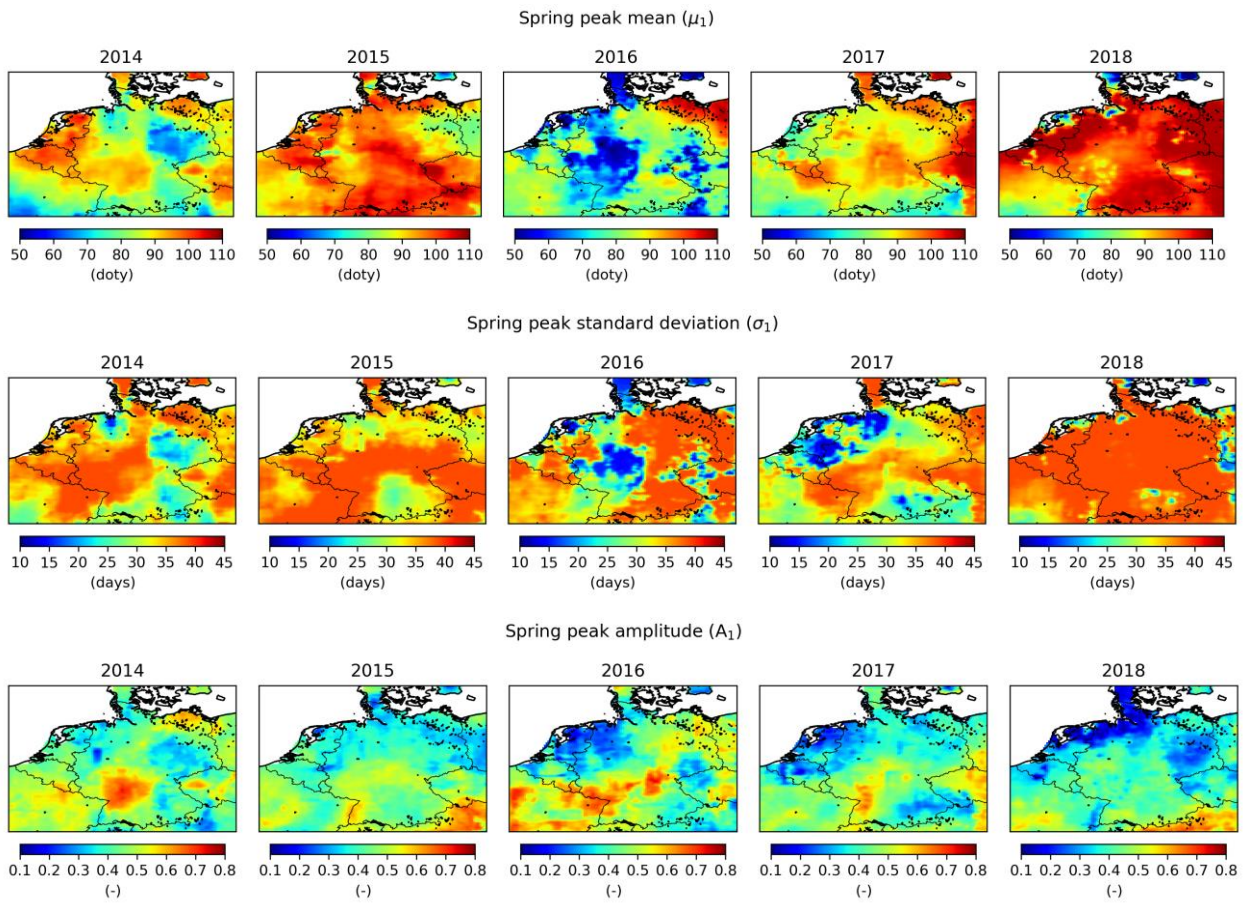


Figure S2: Example of the calculated scaling factors applied to correct for NH_3 surface concentration to NH_3 emission ratios in 2014.



40 **Figure S3: Retrieved (top) and simulated (bottom) NH₃ total column per year.**



45 **Figure S4: The fitted spring peak parameters (μ_1 , σ_1 and A_1) per year.**

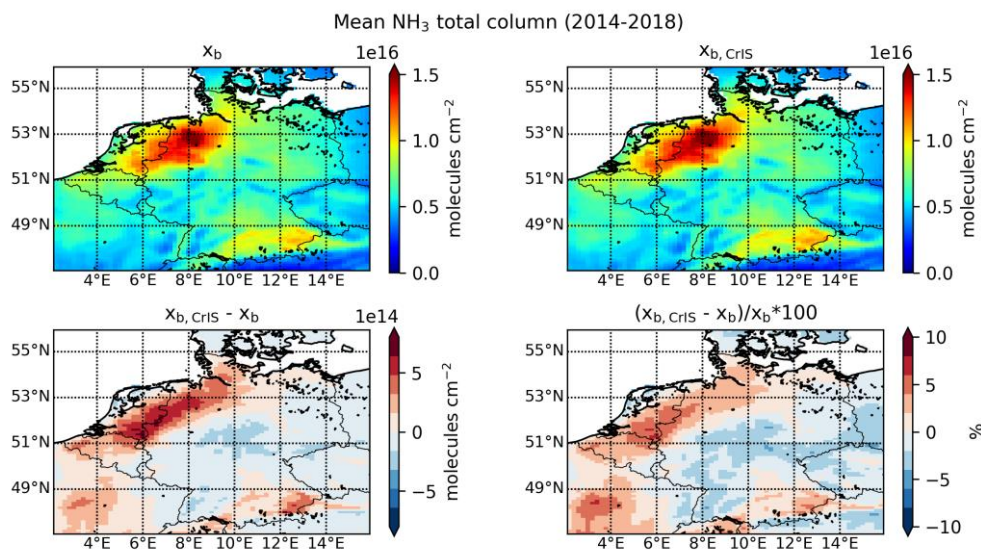


Figure S5: The mean NH₃ total column over 2014 to 2018 from the (top left) default background run (x_b) and the (top right) background run with CrIS-based NH₃ time factors ($x_{b, \text{CrIS}}$) and their (bottom left) absolute and (bottom right) relative difference.

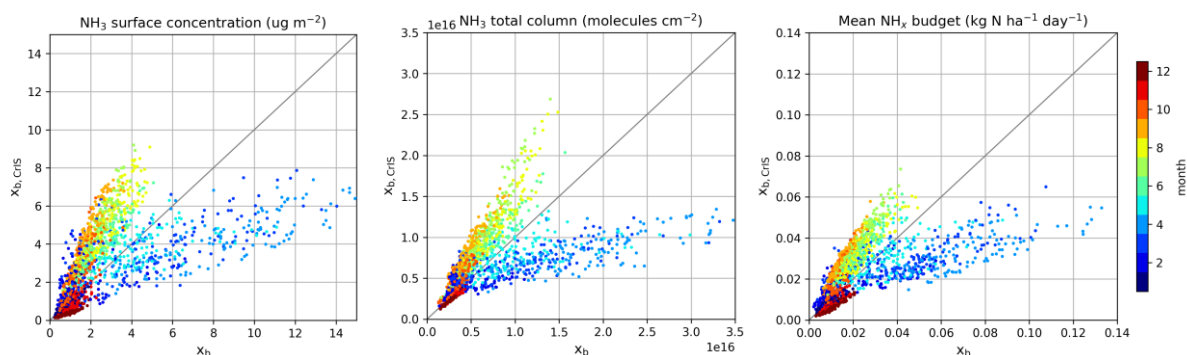


Figure S6: Scatter plots of the daily grid-averaged NH₃ surface concentration (left), NH₃ total column (center) and NH_x deposition (right) colored per month. x_b represents the default LOTOS-EUROS background run and $x_{b, \text{CrIS}}$ the LOTOS-EUROS background run with CrIS-based NH₃ time factors.

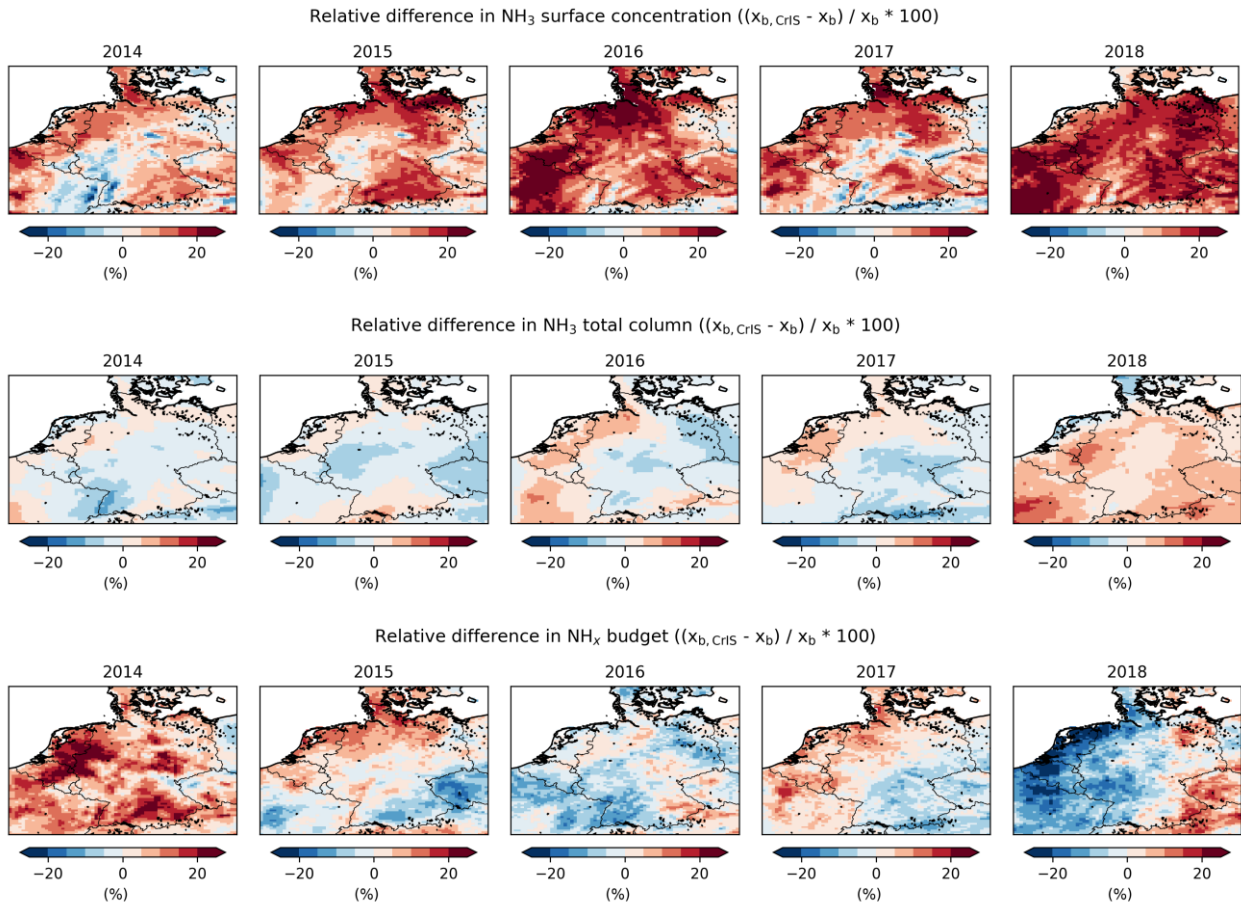


Figure S7: Relative difference in mean NH_3 surface concentrations (top), total column concentrations (center) and total NH_x deposition (bottom) per year following the inclusion of the CrIS-based NH_3 time factors in LOTOS-EUROS. x_b represents the default LOTOS-EUROS background run and $x_{b, \text{CrIS}}$ the LOTOS-EUROS background run with CrIS-based NH_3 time factors.

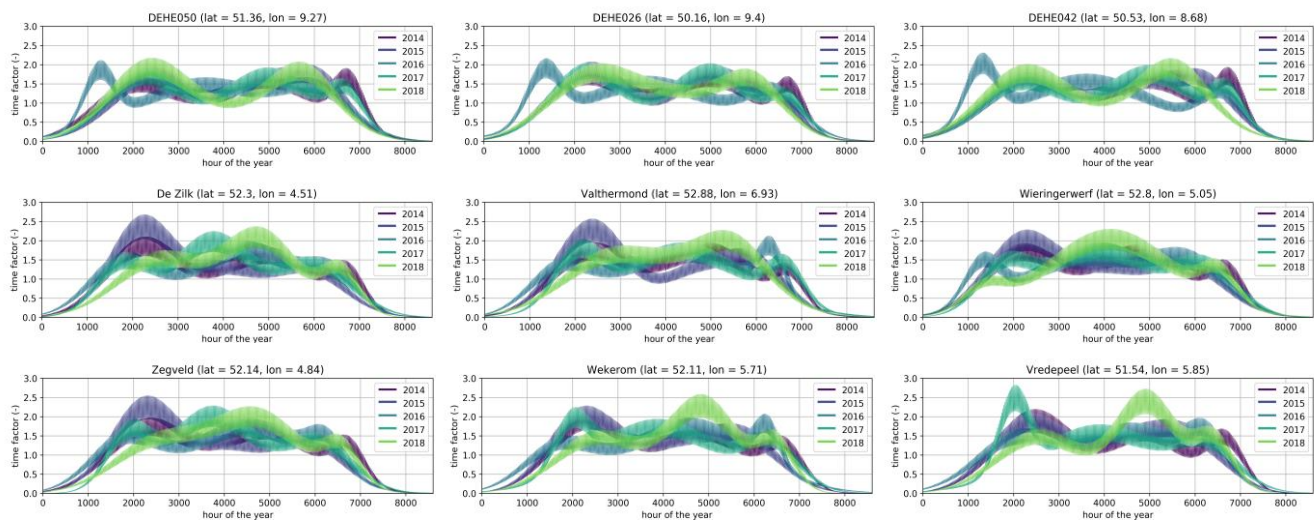


Figure S8: The CrIS-based NH₃ time factors at the hourly observation stations.

Mean NH₃ surface concentration (2014-2018)

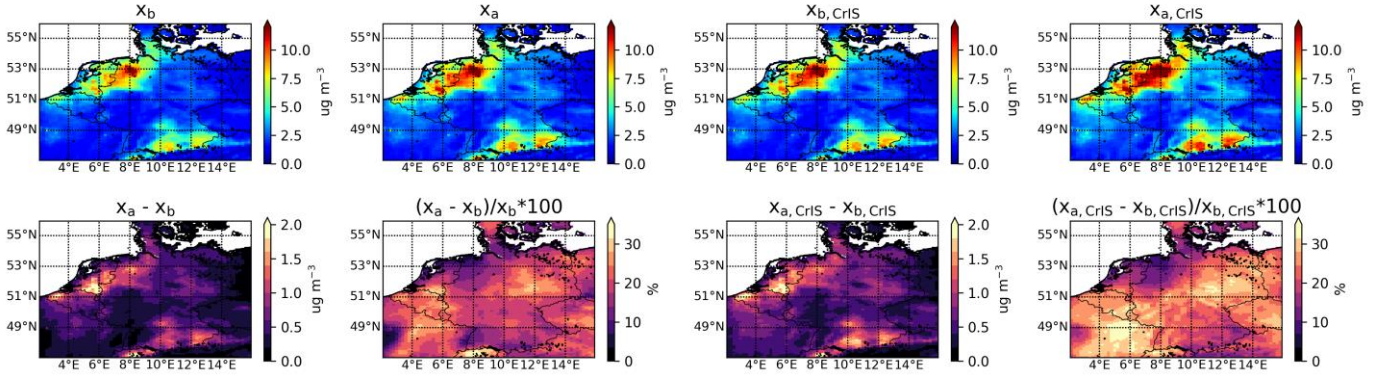


Figure S9: Mean NH₃ surface concentration in 2014-2018 in the background runs x_b and $x_{b,CrIS}$ and in analysis runs x_a and $x_{a,CrIS}$ (top panels), as well as their absolute and relative difference (bottom panels).

80

Mean NH₃ total column (2014-2018)

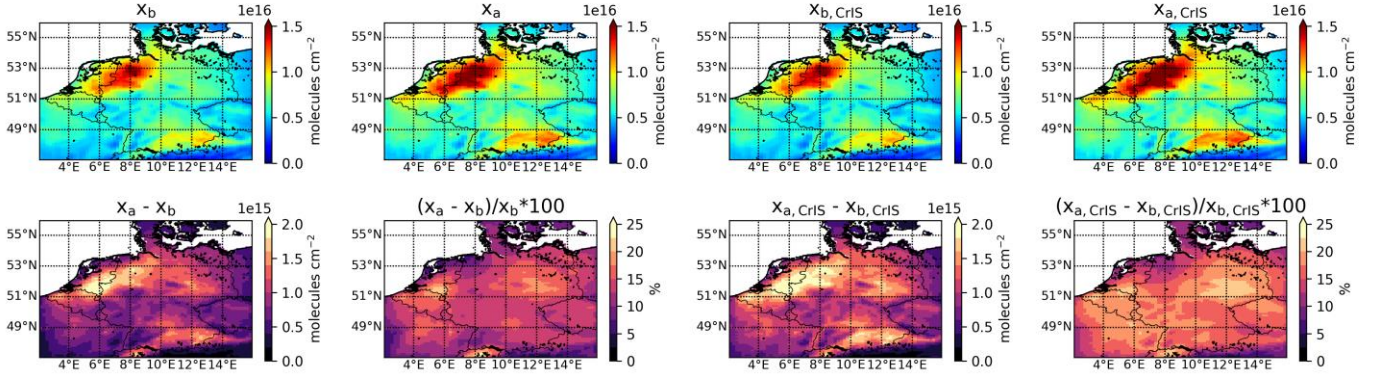


Figure S10: Mean NH₃ total column concentration in 2014-2018 in the background runs x_b and $x_{b,CrIS}$ and in analysis runs x_a and $x_{a,CrIS}$ (top panels), as well as their absolute and relative difference (bottom panels).

85

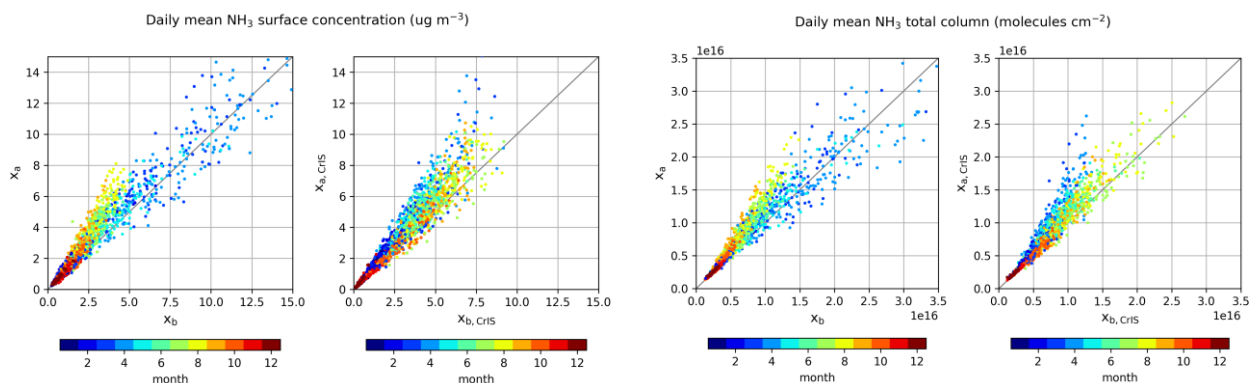
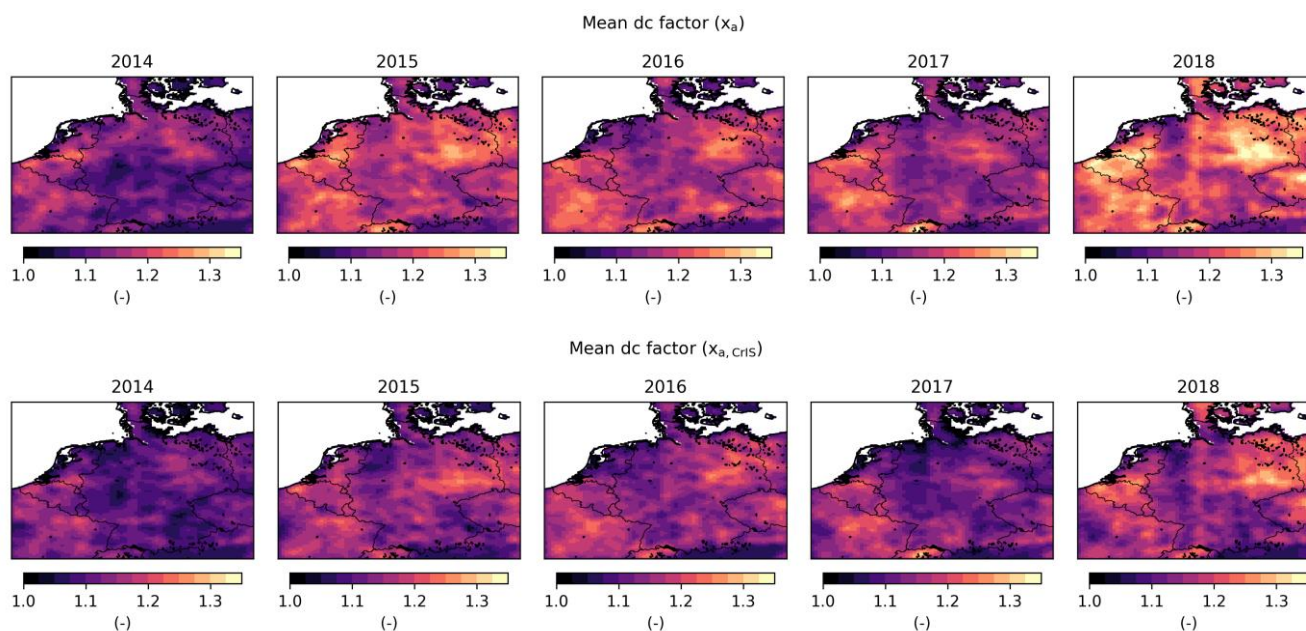
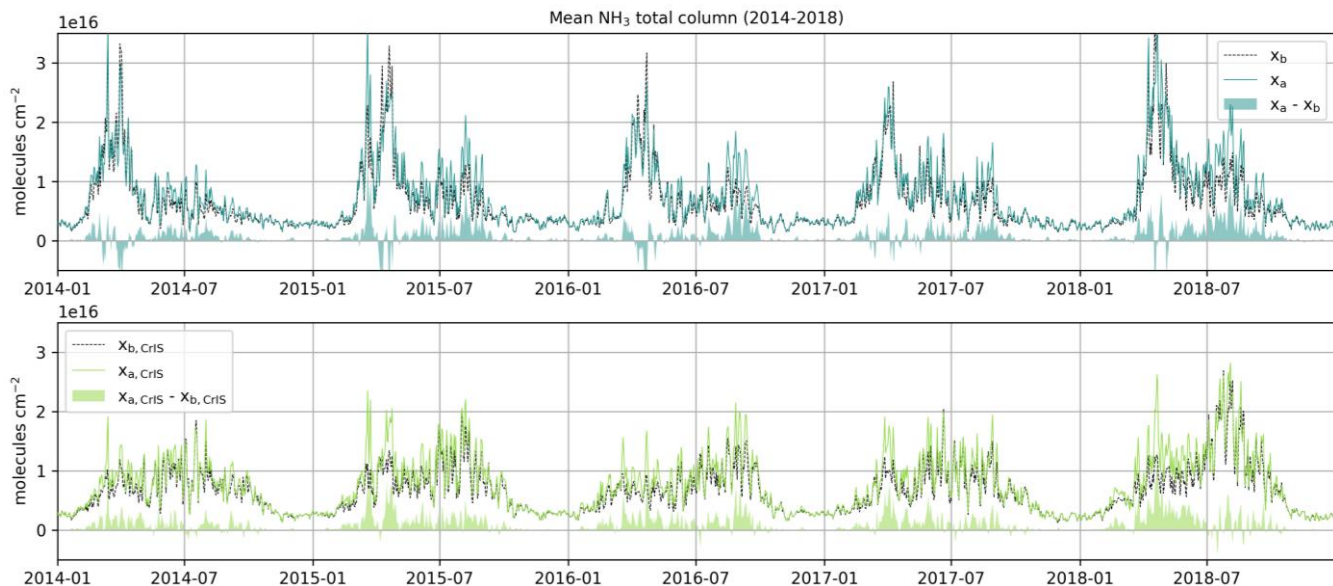


Figure S11: Scatter plots of the daily grid-averaged NH_3 surface concentration (left) and NH_3 total column concentration (right) in 2014-2018 from the background runs x_b and $x_{b, \text{CrIS}}$ versus analysis runs x_a and $x_{a, \text{CrIS}}$ in LOTOS-EUROS, colored per month.

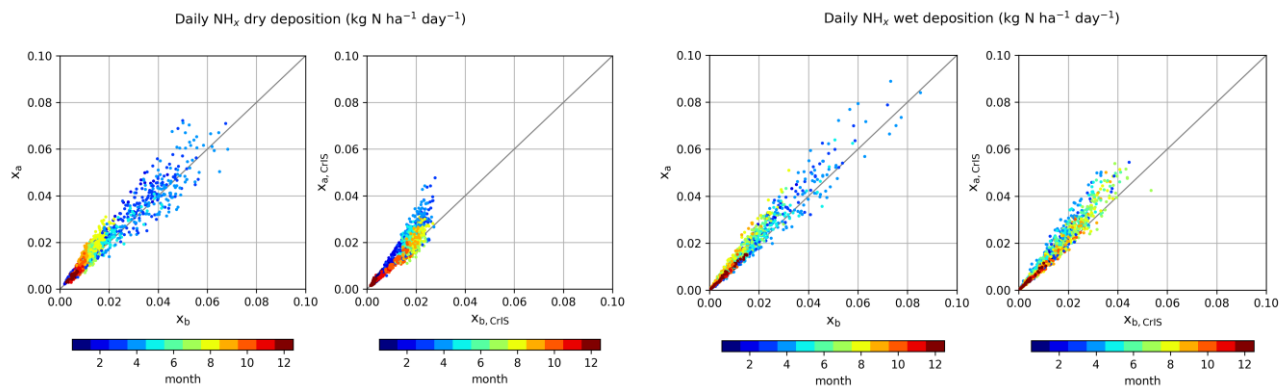


90

Figure S12: Mean emission perturbation factors (β) per year for (top) LOTOS-EUROS runs with default NH_3 emission time factors and (bottom) LOTOS-EUROS runs with CrIS-based NH_3 time factors.



95 **Figure S13: Timeseries of the daily grid-averaged NH_3 total column concentrations in the background and analysis runs, and their absolute difference. The top figure (blue) represents the default background (x_b) and analysis run (x_a). The bottom figure (green) the background ($x_{b,\text{CrIS}}$) and analysis run ($x_{a,\text{CrIS}}$) with the CrIS-based NH_3 time factors.**



100 **Figure S14: Scatter plots of the daily grid-averaged amounts of dry (left) and wet (right) NH_x deposition in 2014-2018 from the background (x_b and $x_{b,\text{CrIS}}$) versus the analysis (x_a and $x_{a,\text{CrIS}}$) model runs in LOTOS-EUROS, colored per month.**

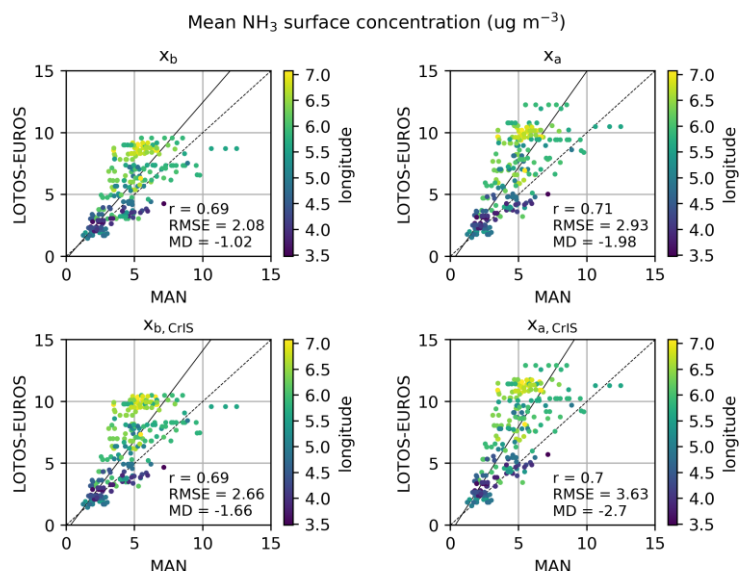


Figure S15: Mean NH_3 surface concentrations (2014-2017) as observed by the Dutch MAN stations and the matching modelled values. The upper figures represent the matching mean NH_3 surface concentrations from the default version of LOTOS-EUROS: x_b the background run and x_a the analysis run. The lower figures represent the matching values from the LOTOS-EUROS run with the CrIS-based NH_3 time factors: $x_{b, \text{CrIS}}$ the background run and $x_{a, \text{CrIS}}$ the analysis run.

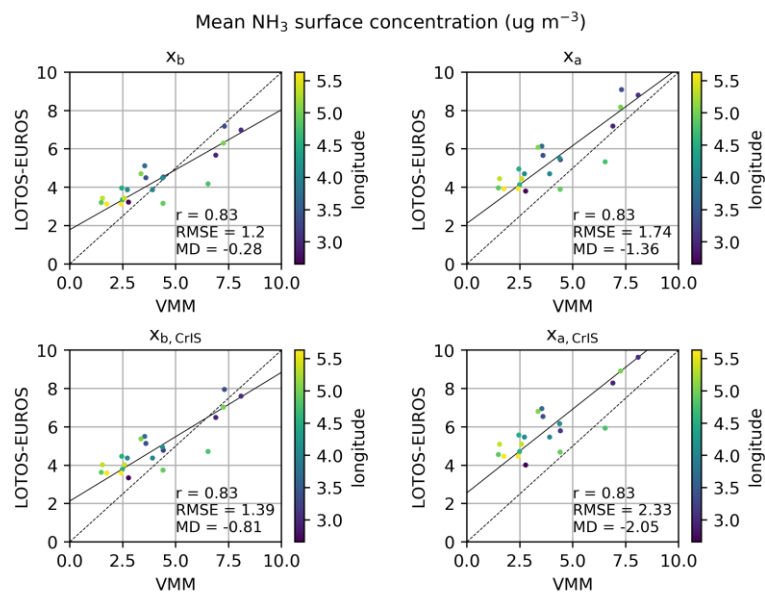


Figure S16: Mean NH_3 surface concentrations (2014-2018) as observed by the Belgium VMM stations and the matching modelled values. The upper figures represent the matching mean NH_3 surface concentrations from the default version of LOTOS-EUROS: x_b the background run and x_a the analysis run. The lower figures represent the matching values from the LOTOS-EUROS run with the CrIS-based NH_3 time factors: $x_{b, \text{CrIS}}$ the background run and $x_{a, \text{CrIS}}$ the analysis run.

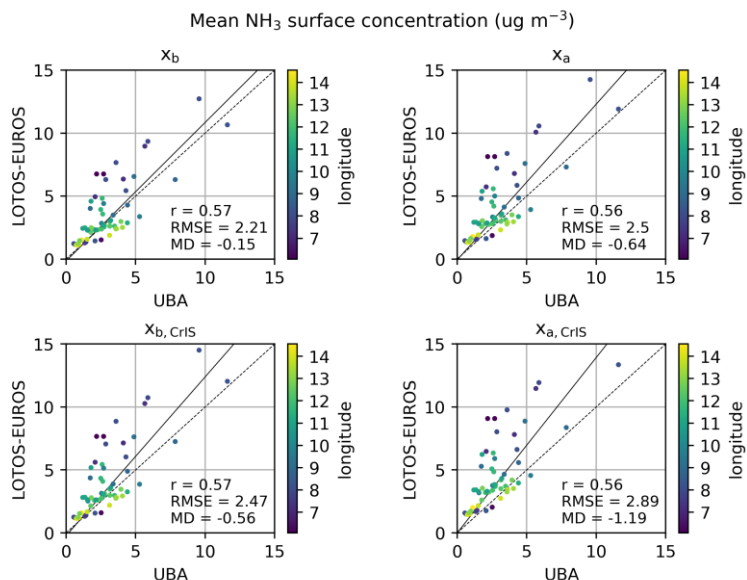


Figure S17: Mean NH_3 surface concentrations (2014-2018) as observed by the German passive sampler stations and the matching modelled values. The upper figures represent the matching mean NH_3 surface concentrations from the default version of LOTOS-EUROS: x_b the background run and x_a the analysis run. The lower figures represent the matching values from the LOTOS-EUROS run with the CrIS-based NH_3 time factors: $x_{b,\text{CrIS}}$ the background run and $x_{a,\text{CrIS}}$ the analysis run.

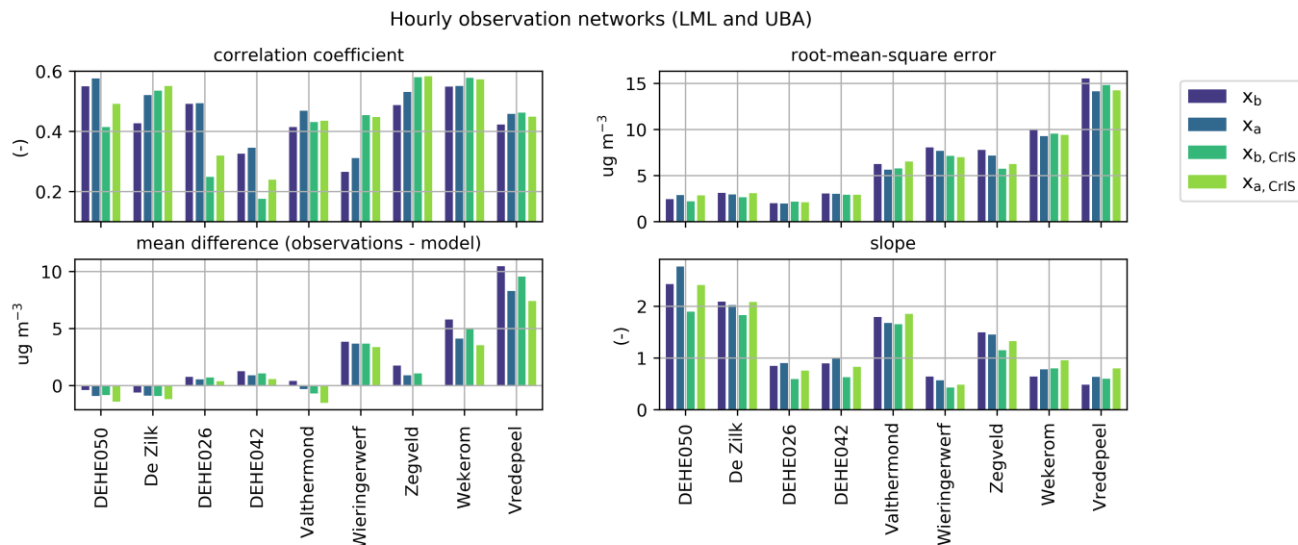


Figure S18: Correlation coefficient r , root-mean-square error, differences in means, slope and intercept between the observed and modelled NH_3 surface concentrations. The stations are sorted by increasing mean NH_3 surface concentration. The colors of the bars represent the different background (x_b and $x_{b,\text{CrIS}}$) and analysis (x_a and $x_{a,\text{CrIS}}$) runs.

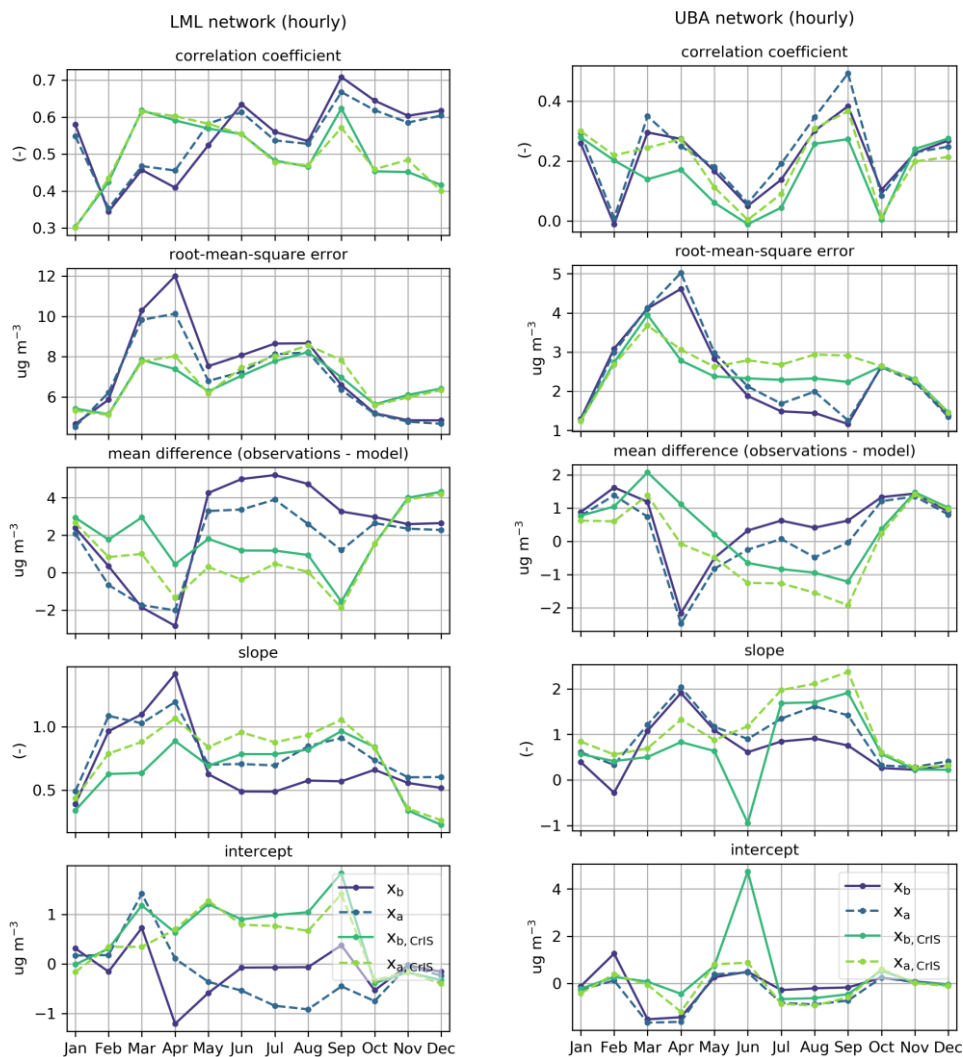
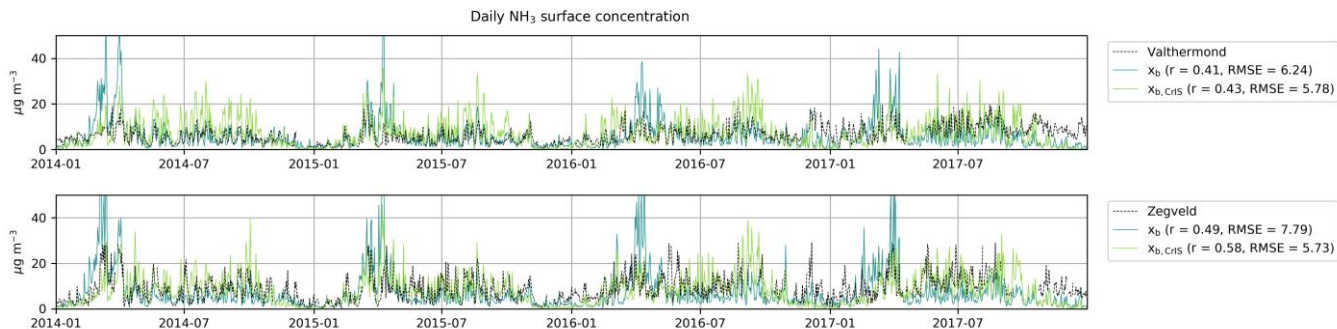


Figure S19: Monthly comparison of the observed and modelled NH_3 surface concentrations per hourly observation network. From top to bottom, the Pearson's correlation coefficient r , the root-mean-square error, the differences in means, the slope and the intercept are plotted. The purple lines represent the default version of LOTOS-EUROS (x_b being the background run, x_a the analysis run) and the green lines the version of LOTOS-EUROS with the CrIS-based NH_3 time factors ($x_{b,\text{CrIS}}$ the background run, $x_{a,\text{CrIS}}$ the analysis run).



130 **Figure S20: Example of the observed and modelled daily NH_3 surface concentrations at LML stations Valthermond and Zegveld. x_b represents the default LOTOS-EUROS background run and $x_{b,\text{CrIS}}$ the LOTOS-EUROS background run with CrIS-based NH_3 time factors.**

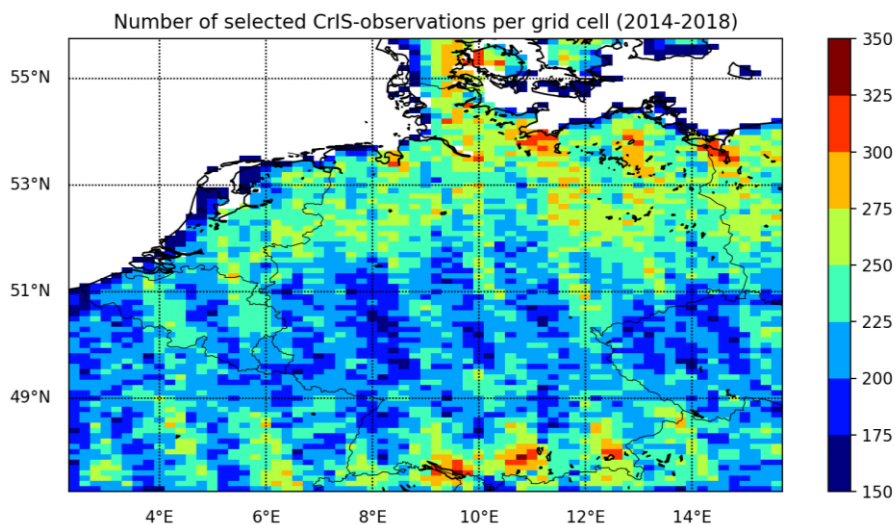


Figure S21: Number of selected CrIS- NH_3 observations per grid cell.

135

140

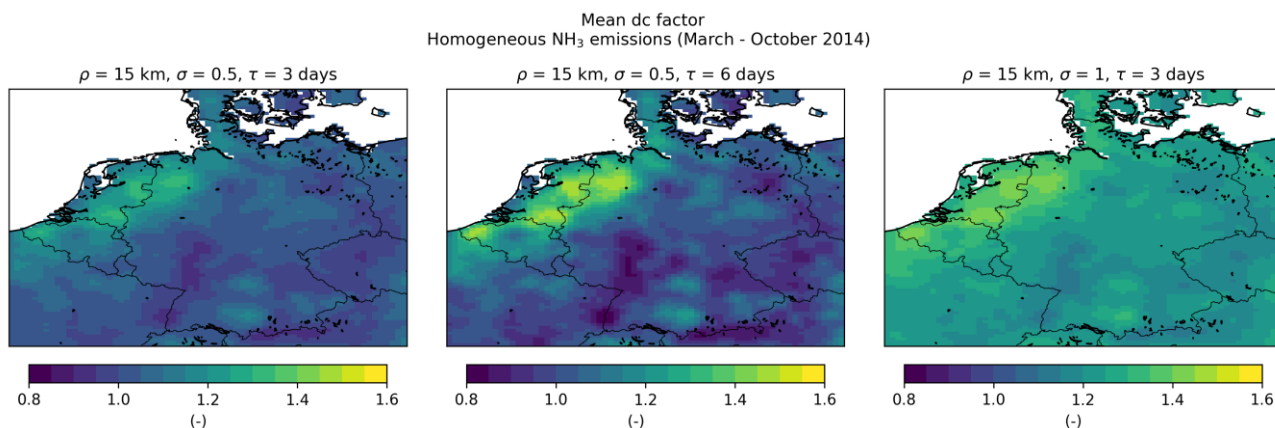


Figure S22: Mean emission perturbation factors (β) from March to October 2014 for model runs with initially homogeneous NH₃ emissions, using different local Ensemble Kalman filter settings.

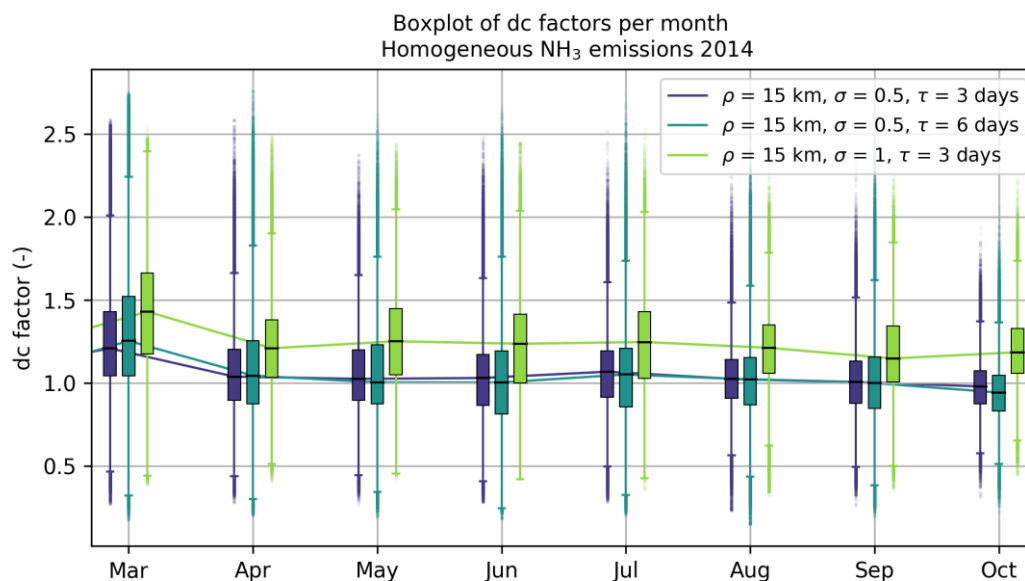
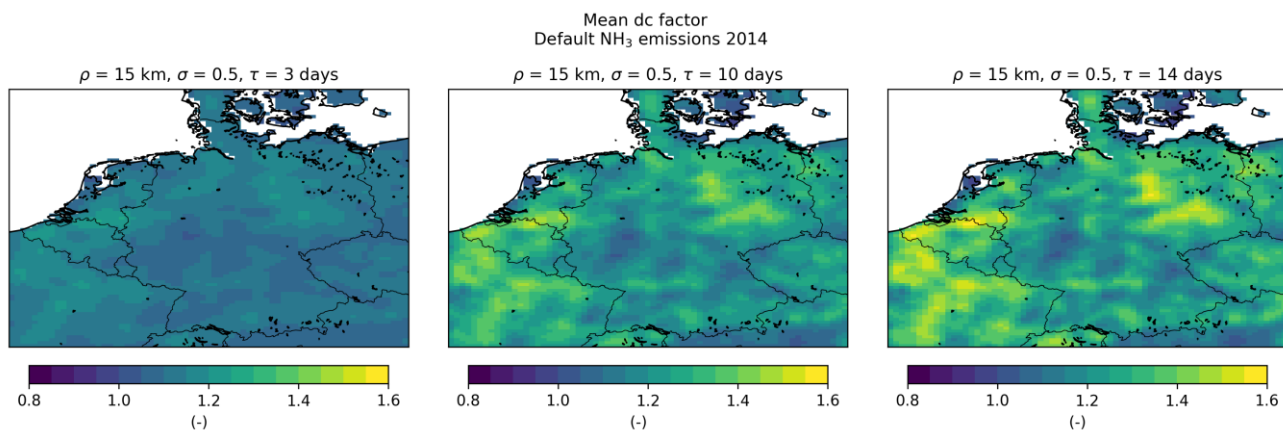


Figure S23: Distribution of emission perturbation factors (β) per month for model runs with initially homogeneous NH₃ emissions, using different local Ensemble Transform Kalman filter settings.



150 **Figure S24:** Mean emission perturbation factors (β) in 2014 for model runs with default NH₃ emissions with varying temporal correlation length τ values.

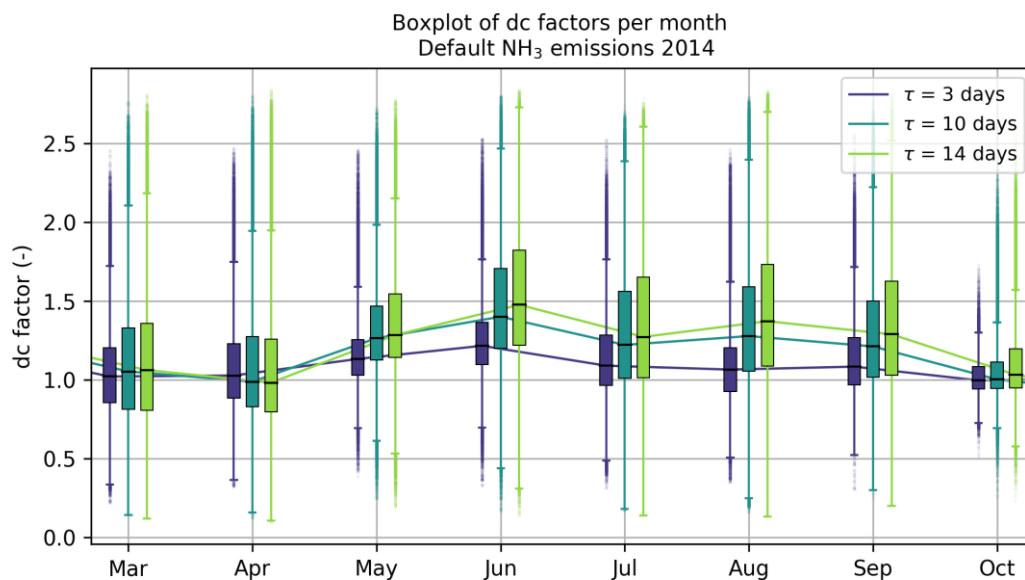


Figure S25: Distribution of emission perturbation factors (β) per month for model runs with default NH₃ emissions, using different values for temporal correlation length τ .